Earthquakes and Structures, *Vol. 15, No. 3 (2018) 285-294*
DOI: https://doi.org/10.12989/eas.2018.15.3.285

Seismic analysis of AL_2O_3 nanoparticles-reinforced concrete plates based on sinusoidal shear deformation theory

Abolfazl Amoli, Reza Kolahchi* and Mahmood Rabani Bidgoli

Department of Civil Engineering, Jasb Branch, Islamic Azad University, Jasb, Iran

(Received June 1, 2018, Revised June 21, 2018, Accepted June 22, 2018)

Abstract. In this study, nonlinear dynamic response of a concrete plate retrofit with Aluminium oxide (Al_2O_3) under seismic load and magnetic field is investigated. The plate is a composite reinforced by Aluminium oxide with characteristics of the equivalent composite being determined using Mori-Tanka model considering agglomeration effect. The plate is simulated with higher order shear deformation plate model. Employing nonlinear strains-displacements, stress-strain, the energy equations of column was obtained and using Hamilton's principal, the governing equations were derived. Differential quadrature method (DQM) in conjunction with Newark method is applied for obtaining the dynamic response of structure. The influences of magnetic field, volume percent of nanoparticles, geometrical parameters of column, agglomeration and boundary conditions on the dynamic response were investigated. Results showed that with increasing volume percent of nanoparticles, the dynamic deflection decreases.

Keywords: dynamic response; nano-composite plate; DQM; magnetic field; seismic load

1. Introduction

Seismic analysis is a subset of structural analysis in which dynamic response of a building structure (or non-building structures such as bridges, etc.) against the earthquake is examined. This analysis is a part of the structural engineering, the earthquake engineering and seismic retrofitting of the structures which should be constructed in earthquake prone zones (Liang and Parra-Montesinos 2004).

Mechanical analysis of nanostructures has been reported by many researchers (Zemri 2015, Larbi Chaht 2015, Belkorissat 2015, Ahouel 2016, Bounouara 2016, Bouafia 2017, Besseghier 2017, Bellifa 2017, Mouffoki 2017, Khetir 2017, Boadu *et al.* 2017). Liang and Parra-Montesinos (2004) studied seismic behavior of four reinforced concrete column-steel plate under various ground motions using experimental tests. Cheng and Chen (2004), Changwang *et al.* (2010) studied seismic behavior of steel reinforced concrete column-steel truss plate. They developed a design formula for shear strength of the structure subjected to seismic activities using experimental tests. The effect of cumulative damage on the seismic behavior of steel tube-reinforced concrete (ST-RC) columns through experimental testing was investigated by Ji *et al.* (2014). Six large-scale ST-RC column specimens were subjected to high axial forces and cyclic lateral loading. The effect of plastic hinge relocation on the potential damage of a reinforced concrete frame subjected to different seismic levels was studied by Cao and Ronagh (2014) based on current seismic designs. The optimal seismic retrofit method that uses FRP jackets for shear-critical RC frames was presented by Choi *et al.* (2014). This optimal method uses non-dominated sorting genetic algorithm-II (NSGA-II) to optimize the two conflicting objective functions of the retrofit cost as well as the seismic performance, simultaneously. They examined various parameters like, failure mode, hysteresis curves, ductility and reduction of stiffness. Liu *et al.* (2016) focused on the study of seismic behavior of steel reinforced concrete special-shaped column-plate joints. Six specimens, which are designed according to the principle of strong-member and weak-joint core, are tested under low cyclic reversed load.

In none of the above articles, the nanocomposite structure is considered. Wuite and Adali (2005) performed stress analysis of carbon nanotubes (CNTs) reinforced plates. They concluded that using CNTs as reinforcing phase can increase the stiffness and the stability of the system. Also, Matsunaga (2007) examined stability of the composite cylindrical shell using third-order shear deformation theory (TSDT). Formica *et al.* (2010) analyzed vibration behavior of CNTs reinforced composites. They employed an equivalent continuum model based onEshelby-Mori-Tanaka model to obtain the material properties of the composite. Liew *et al.* (2014) studied postbuckling of nanocomposite cylindrical panels. They used the extended rule of mixture to estimate the effective material properties of the nanocomposite structure. They also applied a meshless approach to examine the postbuckling response of the nanocomposite cylindrical panel. In another similar work, Lei *et al.* (2014) studied dynamic stability of a CNTs reinforced functionally graded (FG) cylindrical panel. They used Eshelby-Mori-Tanaka model to estimate effective material properties of the resulting nanocomposite structure and also employed Ritz method to distinguish the instability

*Corresponding author, Professor
E-mail: r.kolahchi@iaujasb.ac.ir

ISSN: 2092-7614 (Print), 2092-7622 (Online)

regions of the structure. Static stress analysis of CNTs reinforced cylindrical shells is presented by Ghorbanpour Arani *et al*. (2015). In this work, the cylindrical shell was subjected to non-axisymmetric thermal-mechanical loads and uniform electro-magnetic fields. Eventually, the stress distribution in the structure is determined analytically by Fourier series. Buckling analysis of CNTs reinforced microplates is carried out by Kolahchi *et al*. (2013). They derived the governing equations of the structure based on Mindlin plate theory and using Hamilton's principle. They obtained buckling load of the structure by applying differential quadrature method (DQM). Dynamic response of FG circular cylindrical shells is examined by Davar *et al*. (2013). They developed the mathematical formulation of the structure according to first order shear deformation theory (FSDT) and Love's first approximation theory. Also, Kolahchi *et al*. (2016) investigated dynamic stability of FG-CNTs reinforced plates. The material properties of the plate are assumed to be a function of temperature and the structure is considered resting on orthotropic elastomeric medium. Jafarian Arani and Kolahchi (2016) presented a mathematical model for buckling analysis of a CNTs reinforced concrete column. They simulated the problem based on Euler Bernoulli and Timoshenko plate theories. Nonlinear vibration of laminated cylindrical shells is analyzed by Shen and Yang (2014). They examined the influences of temperature variation, shell geometric parameter and applied voltage on the linear and nonlinear vibration of the structure. An investigation on the nonlinear dynamic response and vibration of the imperfect laminated three-phase polymer nanocomposite panel resting on elastic foundations was presented by Duc *et al*. (2015). Van Thu and Duc (2016) presented an analytical approach to investigate the non-linear dynamic response and vibration of an imperfect three-phase laminated nanocomposite cylindrical panel resting on elastic foundations in thermal environments. Alibeigloo (2016) employed theory of piezo-elasticity to study bending behavior of FG-CNTs reinforced composite cylindrical panels. They used an analytical method to study the effect of CNT volume fraction, temperature variation and applied voltage on the bending behavior of the system. Feng *et al*. (2017) studied the nonlinear bending behavior of a novel class of multi-layer polymer nanocomposite plates reinforced with graphene platelets (GPLs) that are non-uniformly distributed along the thickness direction. Duc *et al*. (2017a, b, c) studied thermal and mechanical stability of a functionally graded composite truncated conical shell, plates and double curved shallow shells reinforced by carbon nanotube fibers. Based on Reddy's third-order shear deformation plate theory, the nonlinear dynamic response and vibration of imperfect functionally graded carbon nanotube-reinforced composite plates was analyzed by Thanh *et al*. (2017). Duc *et al*. (2018) presented the first analytical approach to investigate the nonlinear dynamic response and vibration of imperfect rectangular nanocompsite multilayer organic solar cell subjected to mechanical loads using the classical plate theory.

For the first time, dynamic response of AL_2O_3 nanoparticles-reinforced concrete plates subjected to seismic excitation and magnetic field is studied in the present research. So, the results of this research are of great importance in Civil Engineering. The concrete plate is modeled by applying SSPT and the effective material properties of the concrete plate are obtained based on Mori-Tanaka model considering agglomeration of AL_2O_3 nanoparticles. The dynamic displacement of structure is calculated by HDQM in conjunction with Newmark method. The effects of different parameters such as volume fraction and agglomeration of AL_2O_3 nanoparticles, magnetic field, boundary conditions and geometrical parameters of concrete plate are studied on the dynamic response of the structure.

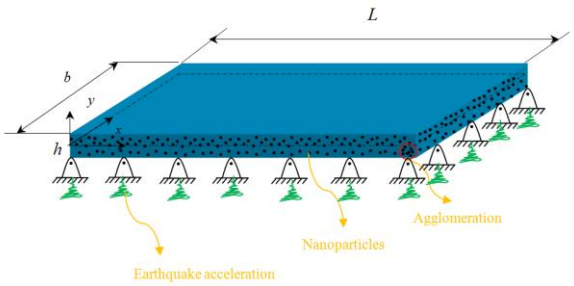

Fig. 1 Schematic figure of concrete plate reinforced by agglomerated AL_2O_3 nanoparticles under magnetic field

2. Formulation

2.1 Strain relations

As shown in Fig. 1, a concrete plate is reinforced by agglomerated AL_2O_3 nanoparticles subjected to the earthquake load and magnetic field. The geometrical parameters of plate are length of L and thickness of h.

There are many new theories for modeling of different structures. Some of the new theories have been used by Tounsi and co-authors (Bessaim 2013, Bouderba 2013, Belabed 2014, Ait Amar Meziane 2014, Zidi 2014, Hamidi 2015, Bourada 2015, Bousahla *et al*. 2016a, b, Beldjelili 2016, Boukhari 2016, Draiche 2016, Bellifa 2015, Attia 2015, Mahi 2015, Ait Yahia 2015, Bennoun 2016, El-Haina 2017, Menasria 2017, Chikh 2017).

By applying SSPT, the displacements fields are defined as below (Simsek and Reddy 2013)

$$\begin{aligned} U_1(x,y,z,t) &= U(x,y,t) - z\frac{\partial W_b}{\partial x} - \Phi(z)\frac{\partial W_s}{\partial x}, \\ U_2(x,y,z,t) &= V(x,y,t) - z\frac{\partial W_b}{\partial y} - \Phi(z)\frac{\partial W_s}{\partial y}, \\ U_3(x,y,z,t) &= W_b(x,y,t) + W_s(x,y,t), \end{aligned} \tag{1}$$

where U, V and W are the respective translation displacements of a point at the mid-plane of the plate in the longitudinal x, transverse y and thickness z directions. Also, ϕ denotes the rotation of the cross section area and $\Phi(z)$ is the shape function of the plate which is considered as follows

$$\Phi(z) = \left(z - \left(\frac{h}{\pi}\sin\frac{\pi z}{h}\right)\right), \tag{2}$$

However, the strain-displacement relations of the structure are given as below

$$\begin{pmatrix}\varepsilon_{xx}\\ \varepsilon_{yy}\\ \gamma_{xy}\end{pmatrix}=\begin{pmatrix}\varepsilon_{xx}^{0}\\ \varepsilon_{yy}^{0}\\ \gamma_{xy}^{0}\end{pmatrix}+z\begin{pmatrix}k_{xx}^{b}\\ k_{yy}^{b}\\ k_{xy}^{b}\end{pmatrix}+\left(z-\frac{h}{\pi}\sin\frac{\pi z}{h}\right)\begin{pmatrix}k_{xx}^{s}\\ k_{yy}^{s}\\ k_{xy}^{s}\end{pmatrix} \tag{3a}$$

$$\begin{pmatrix}\gamma_{yz}\\ \gamma_{xz}\end{pmatrix}=\cos\left(\frac{\pi z}{h}\right)\begin{pmatrix}\gamma_{yz}^{s}\\ \gamma_{xz}^{s}\end{pmatrix} \tag{3b}$$

where

$$\begin{pmatrix}\varepsilon_{xx}^{0}\\ \varepsilon_{yy}^{0}\\ \gamma_{xy}^{0}\end{pmatrix}=\begin{pmatrix}\dfrac{\partial U}{\partial x}\\ \dfrac{\partial V}{\partial y}\\ \dfrac{\partial U}{\partial y}+\dfrac{\partial V}{\partial x}\end{pmatrix},\quad\begin{pmatrix}k_{xx}^{b}\\ k_{yy}^{b}\\ k_{xy}^{b}\end{pmatrix}=\begin{pmatrix}-\dfrac{\partial^2 W_b}{\partial x^2}\\ -\dfrac{\partial^2 W_b}{\partial y^2}\\ -2\dfrac{\partial^2 W_b}{\partial x\,\partial y}\end{pmatrix},\quad\begin{pmatrix}k_{xx}^{s}\\ k_{yy}^{s}\\ k_{xy}^{s}\end{pmatrix}=\begin{pmatrix}-\dfrac{\partial^2 W_s}{\partial x^2}\\ -\dfrac{\partial^2 W_s}{\partial y^2}\\ -2\dfrac{\partial^2 W_s}{\partial x\,\partial y}\end{pmatrix} \tag{4}$$

$$\begin{pmatrix}\gamma_{yz}^{s}\\ \gamma_{xz}^{s}\end{pmatrix}=\frac{-4}{h^3}\begin{pmatrix}\dfrac{\partial W_s}{\partial y}\\ \dfrac{\partial W_s}{\partial x}\end{pmatrix} \tag{5}$$

2.2 Stress relations

The constitutive equations of the orthotropic plate are considered as below

$$\begin{bmatrix}\sigma_{xx}\\ \sigma_{yy}\\ \sigma_{zz}\\ \sigma_{zy}\\ \sigma_{xz}\\ \sigma_{zy}\end{bmatrix}=\begin{bmatrix}C_{11}&C_{12}&C_{13}&0&0&0\\ C_{12}&C_{22}&C_{23}&0&0&0\\ C_{13}&C_{23}&C_{33}&0&0&0\\ 0&0&0&C_{44}&0&0\\ 0&0&0&0&C_{55}&0\\ 0&0&0&0&0&C_{66}\end{bmatrix}\begin{bmatrix}\varepsilon_{xx}\\ \varepsilon_{yy}\\ \varepsilon_{zz}\\ \gamma_{zy}\\ \gamma_{xz}\\ \gamma_{xy}\end{bmatrix}, \tag{6}$$

where C_{ij} are the elastic constants of the concrete plate. To obtain the effective material properties of the concrete plate and to consider the agglomeration effect, Mori-Tanak model (Mori andTanak 1973) is employed which the effective Young's modulus E and Poisson's ratio v of the composite material are given by

$$E=\frac{9KG}{3K+G}\quad, \tag{7}$$

$$\upsilon=\frac{3K-2G}{6K+2G}. \tag{8}$$

where the effective bulk modulus K and shear modulus G may be written as below (Shu and Xue 1997)

$$K=K_{out}\left[1+\frac{\xi\left(\dfrac{K_{in}}{K_{out}}-1\right)}{1+\alpha(1-\xi)\left(\dfrac{K_{in}}{K_{out}}-1\right)}\right]\quad, \tag{9}$$

$$G=G_{out}\left[1+\frac{\xi\left(\dfrac{G_{in}}{G_{out}}-1\right)}{1+\beta(1-\xi)\left(\dfrac{G_{in}}{G_{out}}-1\right)}\right], \tag{10}$$

The agglomeration effect can be considered based on the micro-mechanical model by introducing the two following parameters

$$\xi=\frac{V_{inclusion}}{V}, \tag{11}$$

$$\zeta=\frac{V_r^{inclusion}}{V_r}. \tag{12}$$

where V_r and $V_r^{inclusion}$ are the total volume of nanoparticles and volume of the nanoparticles inside the inclusion, respectively. in addition, K_{in} and K_{out} are the effective bulk modulus of the inclusion and the matrix outside the inclusion, respectively. Also, G_{in} and G_{out} are the effective shear modulus of the inclusion and the matrix outside the inclusion, respectively and are given as follows

$$K_{in}=K_m+\frac{(\delta_r-3K_m\chi_r)C_r\zeta}{3(\xi-C_r\zeta+C_r\zeta\chi_r)}, \tag{13}$$

$$K_{out}=K_m+\frac{C_r(\delta_r-3K_m\chi_r)(1-\zeta)}{3\left[1-\xi-C_r(1-\zeta)+C_r\chi_r(1-\zeta)\right]}, \tag{14}$$

$$G_{in}=G_m+\frac{(\eta_r-3G_m\beta_r)C_r\zeta}{2(\xi-C_r\zeta+C_r\zeta\beta_r)}, \tag{15}$$

$$G_{out}=G_m+\frac{C_r(\eta_r-3G_m\beta_r)(1-\zeta)}{2\left[1-\xi-C_r(1-\zeta)+C_r\beta_r(1-\zeta)\right]}, \tag{16}$$

where C_r is the volume percent of nanoparticles and χ_r, β_r, δ_r and η_r can be obtained as

$$\chi_r=\frac{3(K_m+G_m)+k_r-l_r}{3(k_r+G_m)}, \tag{17}$$

$$\beta_r=\frac{1}{5}\left\{\begin{aligned}&\frac{4G_m+2k_r+l_r}{3(k_r+G_m)}+\frac{4G_m}{(p_r+G_m)}\\ &+\frac{2\left[G_m(3K_m+G_m)+G_m(3K_m+7G_m)\right]}{G_m(3K_m+G_m)+m_r(3K_m+7G_m)}\end{aligned}\right\}, \tag{18}$$

$$\delta_r=\frac{1}{3}\left[n_r+2l_r+\frac{(2k_r-l_r)(3K_m+2G_m-l_r)}{k_r+G_m}\right], \tag{19}$$

$$\eta_r=\frac{1}{5}\left[\begin{aligned}&\frac{2}{3}(n_r-l_r)+\frac{4G_m p_r}{(p_r+G_m)}+\frac{2(k_r-l_r)(2G_m+l_r)}{3(k_r+G_m)}\\ &+\frac{8G_m m_r(3K_m+4G_m)}{3K_m(m_r+G_m)+G_m(7m_r+G_m)}\end{aligned}\right], \tag{20}$$

in which k_r, l_r, n_r, p_r and m_r are Hill's elastic moduli of the

reinforcing phase of the composite material. Furthermore, K_m and G_m are the bulk and shear moduli of the matrix phase which are defined as below

$$K_m = \frac{E_m}{3(1-2\upsilon_m)} \quad , \tag{21}$$

$$G_m = \frac{E_m}{2(1+\upsilon_m)}. \tag{22}$$

where E_m and ν_m are considered as Young's modulus and Poisson's ratio of the concrete plate, respectively. Moreover, α and β in Eqs. (9) and (10) are given as follows

$$\alpha = \frac{(1+\upsilon_{out})}{3(1-\upsilon_{out})} \quad , \tag{23}$$

$$\alpha = \frac{(1+\upsilon_{out})}{3(1-\upsilon_{out})} \quad , \tag{24}$$

$$\upsilon_{out} = \frac{3K_{out} - 2G_{out}}{6K_{out} + 2G_{out}}. \tag{25}$$

2.3 Energy method

The potential strain energy stored in the structure is given as follows

$$U = \frac{1}{2}\int_A \int_{-\frac{h}{2}}^{\frac{h}{2}} \left(\sigma_{xx}\varepsilon_{xx} + \sigma_{yy}\varepsilon_{yy} + \sigma_{xy}\gamma_{xy} + \sigma_{xz}\gamma_{xz} + \sigma_{yz}\gamma_{yz}\right) dzdA \tag{26}$$

Substituting Eqs. (3) and (4) into Eq. (26) we have

$$\begin{aligned} U = \frac{1}{2}\int_A \Bigg(& N_{xx}\frac{\partial U}{\partial x} + N_{xy}\frac{\partial U}{\partial y} + N_{xy}\frac{\partial V}{\partial x} \\ & + N_{yy}\frac{\partial V}{\partial y} + Q_x\frac{\partial W_s}{\partial x} + Q_y\frac{\partial W_s}{\partial y} - M_{xxS}\frac{\partial^2 W_s}{\partial x^2} \\ & - M_{yyS}\frac{\partial^2 W_s}{\partial y^2} - 2M_{xyS}\frac{\partial^2 W_s}{\partial y \partial x} - M_{xxB}\frac{\partial^2 W_b}{\partial x^2} \\ & - M_{yyB}\frac{\partial^2 W_b}{\partial y^2} - 2M_{xyB}\frac{\partial^2 W_b}{\partial y \partial x}\Bigg) \mathrm{dA}, \end{aligned} \tag{27}$$

where

$$\begin{bmatrix} N_{xx} \\ N_{yy} \\ N_{xy} \end{bmatrix} = \int_{-h}^{h} \begin{bmatrix} \sigma_{xx} \\ \sigma_{yy} \\ \sigma_{xy} \end{bmatrix} dz, \tag{28}$$

$$\begin{bmatrix} M_{xxB} \\ M_{yyB} \\ M_{xyB} \end{bmatrix} = \int_{-h}^{h} \begin{bmatrix} \sigma_{xx} \\ \sigma_{yy} \\ \sigma_{xy} \end{bmatrix} z dz, \tag{29}$$

$$\begin{bmatrix} M_{xxS} \\ M_{yyS} \\ M_{xyS} \end{bmatrix} = \int_{-h}^{h} \begin{bmatrix} \sigma_{xx} \\ \sigma_{yy} \\ \sigma_{xy} \end{bmatrix} f dz, \tag{30}$$

$$\begin{bmatrix} Q_x \\ Q_y \end{bmatrix} = \int_{-h}^{h} \begin{bmatrix} \sigma_{xz} \\ \sigma_{yz} \end{bmatrix} p dz. \tag{31}$$

By substituting Eqs. (5)-(8) into Eqs. (28)-(31), the stress resultants of the plate take the following form

$$\begin{aligned} N_{xx} = {} & A_{11}\frac{\partial}{\partial x}U - A_{11z}\frac{\partial^2}{\partial x^2}W_b - A_{11f}\frac{\partial^2}{\partial x^2}W_s \\ & + A_{12}\frac{\partial}{\partial y}V - A_{12z}\frac{\partial^2}{\partial y^2}W_b - A_{12f}\frac{\partial^2}{\partial y^2}W_s, \end{aligned} \tag{32}$$

$$\begin{aligned} N_{yy} = {} & A_{21}\frac{\partial}{\partial x}U - A_{21z}\frac{\partial^2}{\partial x^2}W_b - A_{21f}\frac{\partial^2}{\partial x^2}W_s \\ & + A_{22}\frac{\partial}{\partial y}V - A_{22z}\frac{\partial^2}{\partial y^2}W_b - A_{22f}\frac{\partial^2}{\partial y^2}W_s, \end{aligned} \tag{33}$$

$$\begin{aligned} N_{xy} = {} & A_{44}\frac{\partial}{\partial y}U + A_{44}\frac{\partial}{\partial x}V \\ & - 2A_{44z}\frac{\partial^2}{\partial x \partial y}W_b - 2A_{44f}\frac{\partial^2}{\partial x \partial y}W, \end{aligned} \tag{34}$$

$$Q_x = A_{55g}\frac{\partial}{\partial x}W_s + GA_{55g}\frac{\partial^2}{\partial x \partial t}W_s, \tag{35}$$

$$Q_y = A_{66g}\frac{\partial}{\partial y}W_s + GA_{66g}\frac{\partial^2}{\partial y \partial t}W_s, \tag{36}$$

$$\begin{aligned} M_{xxB} = {} & A_{11z}\frac{\partial}{\partial x}U - B_{11}\frac{\partial^2}{\partial x^2}W_b - A_{11zf}\frac{\partial^2}{\partial x^2}W_s \\ & + A_{12z}\frac{\partial}{\partial y}V - B_{12}\frac{\partial^2}{\partial y^2}W_b - A_{12zf}\frac{\partial^2}{\partial y^2}W_s, \end{aligned} \tag{37}$$

$$\begin{aligned} M_{xxS} = {} & A_{11f}\frac{\partial}{\partial x}U - A_{11zf}\frac{\partial^2}{\partial x^2}W_b - E_{11}\frac{\partial^2}{\partial x^2}W_s \\ & + A_{12f}\frac{\partial}{\partial y}V - A_{12zf}\frac{\partial^2}{\partial y^2}W_b - E_{12}\frac{\partial^2}{\partial y^2}W_s, \end{aligned} \tag{38}$$

$$\begin{aligned} M_{yyB} = {} & A_{21z}\frac{\partial}{\partial x}U - B_{21}\frac{\partial^2}{\partial x^2}W_b - A_{21zf}\frac{\partial^2}{\partial x^2}W_s \\ & + A_{22z}\frac{\partial}{\partial y}V - B_{22}\frac{\partial^2}{\partial y^2}W_b - A_{22zf}\frac{\partial^2}{\partial y^2}W_s, \end{aligned} \tag{39}$$

$$\begin{aligned} M_{yyS} = {} & A_{21f}\frac{\partial}{\partial x}U - A_{21zf}\frac{\partial^2}{\partial x^2}W_b - E_{21}\frac{\partial^2}{\partial x^2}W_s \\ & + A_{22f}\frac{\partial}{\partial y}V - A_{22zf}\frac{\partial^2}{\partial y^2}W_b - E_{22}\frac{\partial^2}{\partial y^2}W_s, \end{aligned} \tag{40}$$

$$\begin{aligned} M_{xyB} = {} & 2A_{44z}\frac{\partial}{\partial y}U + 2A_{44z}\frac{\partial}{\partial x}V \\ & - 2B_{44}\frac{\partial^2}{\partial x \partial y}W_b - 2A_{44zf}\frac{\partial^2}{\partial x \partial y}W_s, \end{aligned} \tag{41}$$

$$\begin{aligned} M_{xyS} = {} & 2A_{44f}\frac{\partial}{\partial y}U + 2A_{44f}\frac{\partial}{\partial x}V \\ & - 2A_{44zf}\frac{\partial^2}{\partial x \partial y}W_b - 2E_{44}\frac{\partial^2}{\partial x \partial y}W_s, \end{aligned} \tag{42}$$

in which

$$\begin{aligned}(A_{11},A_{12},A_{22},A_{44}) &= \int_{-h}^{h}(C_{11},C_{12},C_{22},C_{44})dz \\ &+ \int_{h}^{h+h_f}(Q_{11},Q_{12},Q_{22},Q_{44})dz,\end{aligned} \tag{43}$$

$$\begin{aligned}(A_{11z},A_{12z},A_{22z},A_{44z}) &= \int_{-h}^{h}(C_{11},C_{12},C_{22},C_{44})zdz \\ &+ \int_{h}^{h+h_f}(Q_{11},Q_{12},Q_{22},Q_{44})zdz,\end{aligned} \tag{44}$$

$$\begin{aligned}(A_{11f},A_{12f},A_{22f},A_{44f}) &= \int_{-h}^{h}(C_{11},C_{12},C_{22},C_{44})fdz \\ &+ \int_{h}^{h+h_f}(Q_{11},Q_{12},Q_{22},Q_{44})fdz,\end{aligned} \tag{45}$$

$$\begin{aligned}(A_{11zf},A_{12zf},A_{22zf},A_{44zf}) &= \int_{-h}^{h}(C_{11},C_{12},C_{22},C_{44})zfdz \\ &+ \int_{h}^{h+h_f}(Q_{11},Q_{12},Q_{22},Q_{44})zfdz\end{aligned} \tag{46}$$

$$(A_{55g},A_{66g}) = \int_{-h}^{h}(C_{55},C_{66})gdz + \int_{h}^{h+h_f}(Q_{55},Q_{66})gdz, \tag{47}$$

$$\begin{aligned}(B_{11},B_{12},B_{22},B_{44}) &= \int_{-h}^{h}(C_{11},C_{12},C_{22},C_{44})z^2dz, \\ &+ \int_{h}^{h+h_f}(Q_{11},Q_{12},Q_{22},Q_{44})z^2dz\end{aligned} \tag{48}$$

$$\begin{aligned}(E_{11},E_{12},E_{22},E_{44}) &= \int_{-h}^{h}(C_{11},C_{12},C_{22},C_{44})f^2dz \\ &+ \int_{h}^{h+h_f}(Q_{11},Q_{12},Q_{22},Q_{44})f^2dz,\end{aligned} \tag{49}$$

The kinetic energy of the structure are defined as below

$$K = \frac{\rho}{2}\int\left(\dot{U}_1^2+\dot{U}_2^2+\dot{U}_3^2\right)dV \tag{52}$$

By substituting Eq. (1) into Eq. (52) we have

$$\begin{aligned}K = 0.5\int\Bigg(&I_0\left(\left(\frac{\partial U}{\partial t}\right)^2+\left(\frac{\partial V}{\partial t}\right)^2+\left(\frac{\partial W_b}{\partial t}\right)^2+\left(\frac{\partial W_s}{\partial t}\right)^2\right)? \\ &-2I_1\left(\frac{\partial U}{\partial t}\frac{\partial^2 W_b}{\partial t\partial x}+\frac{\partial V}{\partial t}\frac{\partial^2 W_b}{\partial t\partial y}\right)+I_2\left(\left(\frac{\partial^2 W_b}{\partial t\partial x}\right)^2+\left(\frac{\partial^2 W_b}{\partial t\partial y}\right)^2\right) \\ &+I_3\left(\left(\frac{\partial^2 W_s}{\partial t\partial x}\right)^2+\left(\frac{\partial^2 W_s}{\partial t\partial y}\right)^2\right)\begin{matrix}+2I_4\left(\frac{\partial^2 w_b}{\partial t\partial x}\frac{\partial^2 W_s}{\partial t\partial x}+\frac{\partial^2 W_b}{\partial t\partial y}\frac{\partial^2 W_s}{\partial t\partial y}\right)\\ +2I_5\left(\frac{\partial U}{\partial t}\frac{\partial^2 W_s}{\partial t\partial x}+\frac{\partial V}{\partial t}\frac{\partial^2 W_s}{\partial t\partial y}\right)\end{matrix}\Bigg)dA.\end{aligned} \tag{53}$$

where

$$(I_0,I_1,I_2,J_1,J_1,K_2) = \int_{-h}^{h}\rho\left(1,z,f,zf,z^2,f^2\right). \tag{54}$$

The external work due the earthquake and magnetic field can be calculated as follows (Kolahchi *et al*. 2016)

$$W = \int(ma(t)+\mu \mathrm{H}_x^2\, h\frac{\partial^2 w}{\partial x^2})Wdx, \tag{56}$$

where m and $a(t)$ are the mass and acceleration of the earth, respectively; μ and H_x are magnetic permeability and magnetic field, respectively. To extract the governing equations of motion, Hamilton's principle is expressed as follows

$$\int_0^t(\delta U-\delta K-\delta W)dt = 0, \tag{57}$$

where δ denotes the variational operator. Substituting Eqs. (58)-(60) into Eq. (57), the motion equations of the structure are obtained as follows

$$\frac{\partial}{\partial x}N_{xx}+\frac{\partial}{\partial y}N_{xy}-I_0\frac{\partial^2 U}{\partial t^2}+I_1\frac{\partial^3 W_b}{\partial x\partial t^2}+J_1\frac{\partial^3 W_s}{\partial x\partial t^2} = 0, \tag{58}$$

$$\frac{\partial}{\partial x}N_{xy}+\frac{\partial}{\partial y}N_{yy}-I_0\frac{\partial^2 V}{\partial t^2}+I_1\frac{\partial^3 W_b}{\partial y\partial t^2}+J_1\frac{\partial^3 W_s}{\partial y\partial t^2} = 0, \tag{59}$$

$$\begin{aligned}&\frac{\partial^2}{\partial x^2}M_{xxB}+2\frac{\partial^2}{\partial x\,\partial y}M_{xyB}+\frac{\partial^2}{\partial y^2}M_{yyB}-K_w w \\ &-I_0\left(\frac{\partial^2 W_b}{\partial t^2}+\frac{\partial^2 W_s}{\partial t^2}\right)-I_1\left(\frac{\partial^3 U}{\partial x\,\partial t^2}+\frac{\partial^3 V}{\partial y\,\partial t^2}\right) \\ &+I_2\left(\frac{\partial^4 W_b}{\partial x^2\partial t^2}+\frac{\partial^4 W_b}{\partial y^2\partial t^2}\right)+J_2\left(\frac{\partial^4 W_s}{\partial x^2\partial t^2}+\frac{\partial^4 W_s}{\partial y^2\partial t^2}\right) = 0,\end{aligned} \tag{60}$$

$$\begin{aligned}&\frac{\partial^2}{\partial x^2}M_{xxS}+2\frac{\partial^2}{\partial x\,\partial y}M_{xyS}+\frac{\partial^2}{\partial y^2}M_{yyS}+\frac{\partial}{\partial x}Q_x \\ &+\frac{\partial}{\partial y}Q_y-K_w w-I_0\left(\frac{\partial^2 W_b}{\partial t^2}+\frac{\partial^2 W_s}{\partial t^2}\right) \\ &-J_1\left(\frac{\partial^3 U}{\partial x\,\partial t^2}+\frac{\partial^3 V}{\partial y\,\partial t^2}\right)+J_2\left(\frac{\partial^4 W_b}{\partial x^2\partial t^2}+\frac{\partial^4 W_b}{\partial y^2\partial t^2}\right) \\ &+K_2\left(\frac{\partial^4 W_s}{\partial x^2\partial t^2}+\frac{\partial^4 W_s}{\partial y^2\partial t^2}\right) = 0,\end{aligned} \tag{61}$$

Also, the boundary conditions of the structure are considered as below

- **Clamped-Clamped supported**

$$\begin{aligned}&W_s = W_b = U = V = \frac{\partial W_s}{\partial x} = \frac{\partial W_b}{\partial x} = 0, @ \quad x = 0, L \\ &W_s = W_b = U = V = \frac{\partial W_s}{\partial x} = \frac{\partial W_b}{\partial x} = 0. \ @ \quad y = 0, b\end{aligned} \tag{62}$$

- **Clamped-Simply supported**

$$\begin{aligned}&W_s = W_b = U = V = \frac{\partial W_s}{\partial x} = \frac{\partial W_b}{\partial x}, @ \quad x = 0, L \\ &W_s = W_b = U = V = M_{xxB} = M_{xxs}. @ \quad y = 0, b\end{aligned} \tag{63}$$

- **Simply-Simply supported**

$$\begin{aligned}&W_s = W_b = U = V = M_{yyB} = M_{yys}, @ \quad x = 0, L \\ &W_s = W_b = U = V = M_{xxB} = M_{xxs}. @ \quad y = 0, b\end{aligned} \tag{64}$$

5. Solution procedure

In this study, DQM is applied to examine the dynamic behavior of the structure. In this numerical method, the governing differential equations of the structure turn into a set of first order algebraic equations by applying the weighting coefficients. According to DQ method, a derivative of a function at a given discrete point will be approximated as a weighted linear sum of the function values at all discrete points chosen in the solution domain. The one-dimensional derivative of the function can be expressed as follows (Kolahchi *et al*. 2016)

$$\frac{d^n f(x_i)}{dx^n} = \sum_{j=1}^{N} C_{ij}^{(n)} f(x_j) \qquad n = 1,...,N-1. \tag{65}$$

where $f(x)$ is the mentioned function, N denotes number of grid points, x_i is a sample point of the function domain, f_i is the value of the function at ith sample point and C_{ij} indicates the weighting coefficients. So, choosing the grid points and weighting coefficients is an important factor in the accuracy of the results. The grid points are considered by Chebyshev polynomials as follows

$$X_i = \frac{L}{2}\left[1-\cos\left(\frac{i-1}{N_x-1}\right)\pi\right] \qquad i = 1,...,N_x \tag{66a}$$

$$y_i = \frac{b}{2}\left[1-\cos\left(\frac{i-1}{N_y-1}\right)\pi\right] \quad i = 1,...,N_y \tag{66b}$$

Based on Chebyshev polynomials, the grid points are closer together near the borders and in distant parts of the borders they away from each other. The weighting coefficients may be calculated by the following simple algebraic relations

$$A_{ij}^{(1)} = \begin{cases} \dfrac{M(x_i)}{(x_i-x_j)M(x_j)} & for \quad i \neq j, \quad i,j = 1,2,...,N_x \\ -\sum\limits_{\substack{j=1 \\ i\neq j}}^{N_x} A_{ij}^{(1)} & for \quad i = j, \quad i,j = 1,2,...,N_x \end{cases} \tag{67a}$$

$$B_{ij}^{(1)} = \begin{cases} \dfrac{P(y_i)}{(y_i-y_j)P(y_j)} & for \quad i \neq j, \quad i,j = 1,2,...,N_y, \\ -\sum\limits_{\substack{j=1 \\ i\neq j}}^{N_y} B_{ij}^{(1)} & for \quad i = j, \quad i,j = 1,2,...,N_y \end{cases} \tag{67a}$$

in which

$$M(x_i) = \prod_{\substack{j=1 \\ j\neq i}}^{N_x} (x_i - x_j) \tag{68a}$$

$$P(y_i) = \prod_{\substack{j=1 \\ j\neq i}}^{N_y} (y_i - y_j) \tag{68b}$$

By distributing the grid points in the domain by substituting Eq. (65) into the governing equations, we have

$$\left(\left[\underbrace{K_L + K_{NL}}_{K}\right]\begin{Bmatrix}\{d_b\}\\ \{d_d\}\end{Bmatrix} + [M]\begin{Bmatrix}\{\ddot{d}_b\}\\ \{\ddot{d}_d\}\end{Bmatrix}\right) = \begin{Bmatrix}\{0\}\\ -Ma(t)\end{Bmatrix}, \tag{69}$$

in which $[K_L]$, $[K_{NL}]$ and $[M]$ indicate linear part of the stiffness matrix, nonlinear part of the stiffness matrix and the mass matrix, respectively. Also, $\{d_b\}$ and $\{d_d\}$ denote boundary and domain points, respectively. To obtain the time response of the structure subjected to the earthquake loads Newmark method (Simsek 2010) is applied in the time domain. Based on this method, Eq. (69) is considered in the general form as below

$$K^*(d_{i+1}) = Q_{i+1}, \tag{70}$$

where subscript i+1 denotes the time $t=t_{i+1}$, $K^*(d_{i+1})$ and Q_{i+1} are the effective stiffness matrix and the effective load vector which are given as

$$K^*(d_{i+1}) = K_L + K_{NL}(d_{i+1}) + \alpha_0 M + \alpha_1 C, \tag{71}$$

$$\begin{aligned} Q_{i+1}^* &= Q_{i+1} + M\left(\alpha_0 d_i + \alpha_2 \dot{d}_i + \alpha_3 \ddot{d}_i\right) \\ &+ C\left(\alpha_1 d_i + \alpha_4 \dot{d}_i + \alpha_5 \ddot{d}_i\right), \end{aligned} \tag{72}$$

where (Simsek 2010)

$$\begin{aligned} &\alpha_0 = \frac{1}{\chi \Delta t^2}, \quad \alpha_1 = \frac{\gamma}{\chi \Delta t}, \quad \alpha_2 = \frac{1}{\chi \Delta t}, \\ &\alpha_3 = \frac{1}{2\chi} - 1, \quad \alpha_4 = \frac{\gamma}{\chi} - 1, \alpha_5 = \frac{\Delta t}{2}\left(\frac{\gamma}{\chi} - 2\right), \\ &\alpha_6 = \Delta t\left(1-\gamma\right), \qquad \alpha_7 = \Delta t \gamma, \end{aligned} \tag{73}$$

where γ=0.5 and χ=0.25. By applying the iteration method, Eq. (70) is solved at any time step and modified velocity and acceleration vectors are computed as follows

$$\ddot{d}_{i+1} = \alpha_0(d_{i+1} - d_i) - \alpha_2 \dot{d}_i - \alpha_3 \ddot{d}_i, \tag{74}$$

$$\dot{d}_{i+1} = \dot{d}_i + \alpha_6 \ddot{d}_i + \alpha_7 \ddot{d}_{i+1}, \tag{75}$$

Then for the next time step, the modified velocity and acceleration vectors in Eqs. (74) and (75) are applied and all the mentioned procedures are repeated.

6. Numerical results

In this section, the effect of various parameters on the dynamic response of the concrete plate reinforced by AL2O3 nanoparticles under seismic load and magnetic field is examined. The length and thickness of the concrete plate are L=3 m and h=15 cm, respectively. The elastic moduli of concrete and AL_2O_3 nanoparticles are E_c=20 GPa and E_r=165 GPa, respectively. The earthquake acceleration is considered based on Kobe earthquake that the distribution of acceleration in 30 seconds is shown in Fig. 2.

6.1 Convergence of DQM

Fig. 3 shows the convergence of DQM in evaluating the maximum deflection of the structure versus time. As it can be seen, with increasing the number of grid points N, the maximum deflection of the structure decreases until N=15, which the results converge to a constant value. So, the results presented below are based on the number of grid

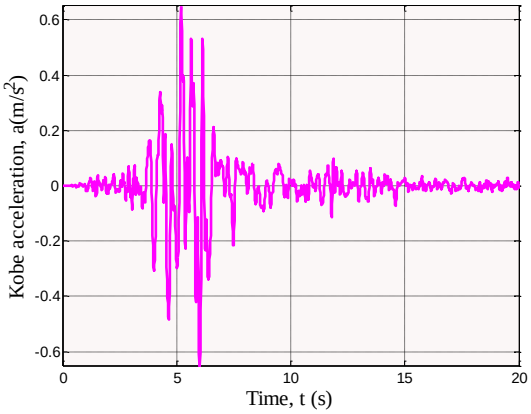

Fig. 2 Acceleration of Kobe

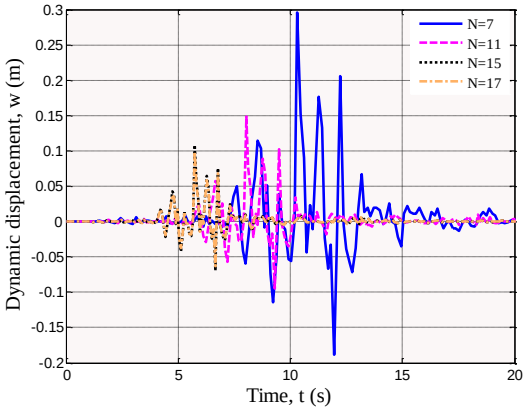

Fig. 3 Convergence and accuracy of DQM

points 15 for DQ solution method.

6.2 Validation of results

Since, there is not any similar work in the literature in the scope of this paper, however, validation of this work is done by comparing the numerical and analytical solutions. The results of the analytical and numerical (DQ) methods are depicted in Fig. 4. As it can be observed, the results of numerical and analytical methods are identical and therefore, the obtained results are accurate and acceptable.

6.3 Effect of magnetic field

Fig. 5 illustrate the effect of magnetic field on the dynamic deflection versus time. As it can be observed, the structure without magnetic field has a greater dynamic deflection with respect to the concrete plate subjected to magnetic field. The reason is that the magnetic field increases the stiffness of the structure. Fig. 5(a) shows the maximum dynamic deflection of the structure without magnetic field equal to 39 while by applying the magnetic field of 1, 5 and 10 A/m, the maximum dynamic displacement of the structure is 27.05, 18.15 and 17.97, respectively. By comparing the results, we can say that applying the magnetic field of 1, 5 and 10 A/m decreases the maximum dynamic displacement of the structure up to 30.64, 53.46 and 53.92 percent which is a remarkable result

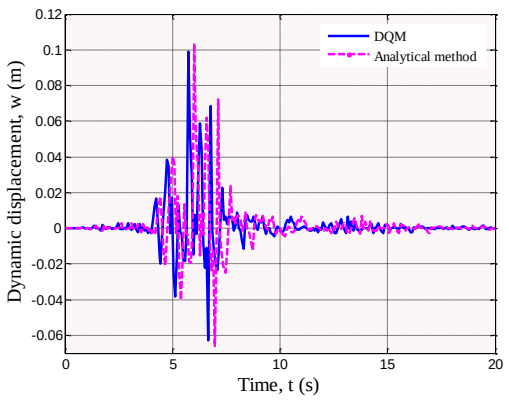

Fig. 4 Comparison of numerical and analytical results

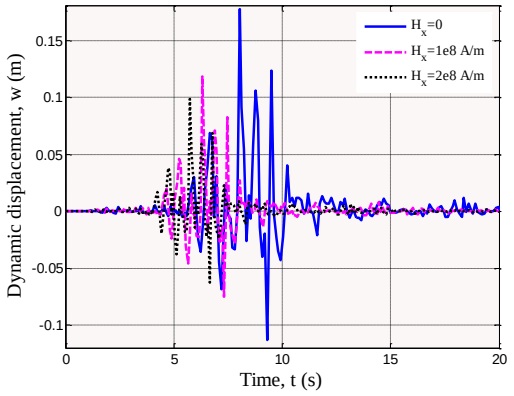

Fig. 5 The effect of magnetic field on the dynamic response of the structure

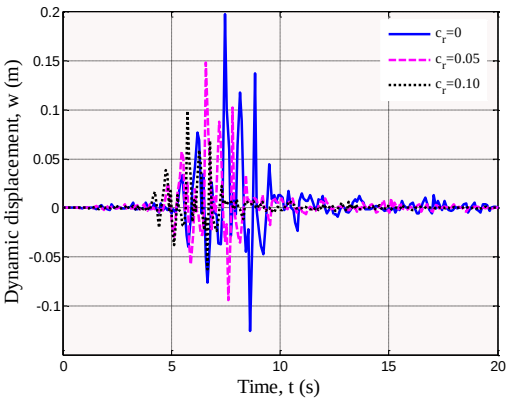

Fig. 6 The effect of AL_2O_3 nanoparticles volume percent on the dynamic response of the structure

in the dynamic designing of the structures. Also it should be noted that the excessive increasing of the magnetic field increases costs while it does not have a noticeable effect on the dynamic response of the structure. Hence, the magnetic field of 5 A/m is the best choice for the present structure.

6.4 Effect of AL2O3 nanoparticles

The effect of AL_2O_3 nanoparticles volume percent on the dynamic response of the structure is studied. Fig. 6(a)-(d). It is apparent that the maximum dynamic displacement of the structure is equals to 32.3 for the case of c_r=0

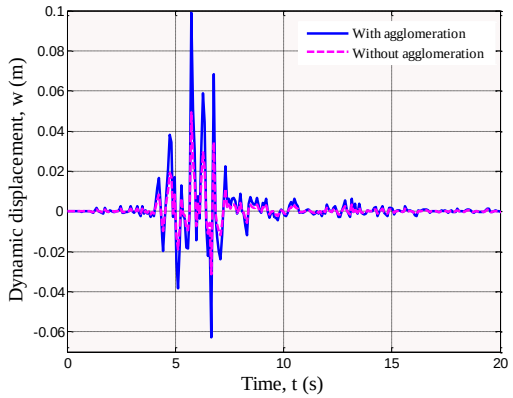

Fig. 7 The effect of AL_2O_3 nanoparticles agglomeration on the dynamic response of the structure

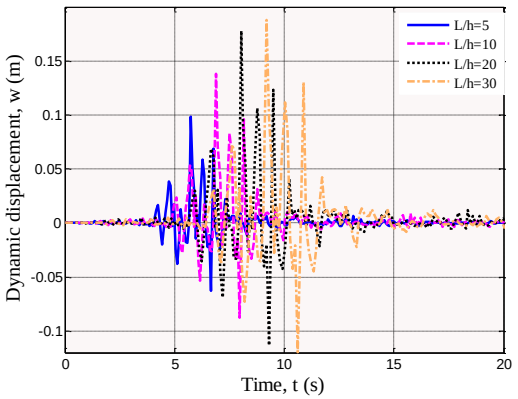

Fig. 8 The effect of concrete plate length on the dynamic response of the structure

(without AL_2O_3 nanoparticles). By using AL2O3 nanoparticles with volume fractions of 0.05, 0.1 and 0.18, the amount of maximum dynamic displacement is 29.1, 27.05 and 30.83, respectively. Therefore, using AL2O3 nanoparticles with volume fractions of 0.05 and 0.1 increases the stiffness of the structure and reduces the maximum displacement of structure 9.91 and 16.25 percent, respectively while the volume percent of 0.18 has a converse result and 4.5 percent increase the deflection.

The agglomeration effect of AL_2O_3 nanoparticles on the dynamic deflection of the structure versus time is illustrated in Fig. 7. As it can be observed, by considering the agglomeration effect, the stiffness of the structure reduces while the dynamic displacement increases. For example, in the absence of the agglomeration effect (ξ=1), the maximum dynamic deflection of the structure is 22.22 while for ξ=0.5 the maximum dynamic deflection is 27.05. The results reveal that the existence of the agglomeration changes the maximum dynamic displacement of the structure up to 21.74 percent.

6.5 Effect of concrete plate length

The effect of concrete plate length on the dynamic response versus time is shown in Fig. 8(a)-(d). It can be seen that with an increase in the concrete plate length, the structure becomes softer and the dynamic deflection of the

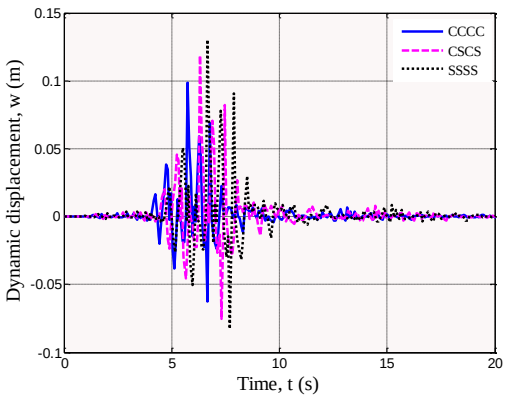

Fig. 9 The effect of different boundary conditions on the dynamic response of the structure

system increases. For example, the maximum dynamic displacements of the concrete plate increase 72.75% with increasing the length from 2 to 3 m.

6.6 Effect of boundary conditions on dynamic response

Fig. 9 illustrate the effect of various boundary conditions on the dynamic response versus time. Four boundary conditions including clamped-clamped, clamped-simply, simply-simply and free-simply supported are considered. The maximum dynamic deflections of the structure for clamped-clamped, clamped-simply supported, simply-simply supported and free-simply supported boundary conditions are 13.53, 18.94, 27.05 and 32.46, respectively. As it can be observed, boundary conditions have a significant effect on the dynamic response of the system so that the structure with clamped-clamped boundary condition has the lowest displacement with respect to the other boundary conditions.

7. Conclusions

Seismic response of concrete plates reinforced by AL_2O_3 nanoparticles was presented in this article. The structure was subjected to axial magnetic field for controlling the dynamic deflection of the structure. Based on SSPT, the structure was simulated and utilizing the energy method and Hamilton's principle, the motion equations were derived. For calculating the effective material properties of structure and considering agglomeration of AL_2O_3 nanoparticles, Mori-Tanaka model was used. Applying HDQ and Newmark methods, the dynamic deflection of the structure was calculated and the effects of different parameters of AL_2O_3 nanoparticles volume percent and agglomeration, magnetic field, boundary conditions and length of the concrete plate were considered on the results. Numerical results indicate that the structure without magnetic field has a greater dynamic deflection with respect to the concrete plate subjected to magnetic field so that applying the magnetic field of 5 A/m decreases the maximum dynamic displacement of the structure up to 53.46 percent. Also it

should be noted that the excessive increasing of the magnetic field increases costs while it does not have a noticeable effect on the dynamic response of the structure. Using AL_2O_3 nanoparticles with volume fractions of 0.05 and 0.1 increases the stiffness of the structure and reduces the maximum displacement of structure 9.91 and 16.25 percent, respectively while the volume percent of 0.18 has a converse result and 4.5 percent increase the deflection. The results reveal that the existence of the agglomeration changes the maximum dynamic displacement of the structure up to 21.74 percent. In addition, the maximum dynamic displacements of the concrete plate increase 72.75% with increasing the length from 2 to 3 m. Furthermore, boundary conditions have a significant effect on the dynamic response of the system so that the structure with clamped-clamped boundary condition has the lowest displacement with respect to the other boundary conditions.

References

Ahouel, M., Houari, M.S.A., Adda Bedia, E.A. and Tounsi A. (2016), "Size-dependent mechanical behavior of functionally graded trigonometric shear deformable nanobeams including neutral surface position concept", *Steel Compos. Struct*., **20**(5), 963-981.

Alibeigloo, A. (2016), "Thermoelastic analysis of functionally graded carbon nanotube reinforced composite cylindrical panel embedded in piezoelectric sensor and actuator layers", *Compos. Part B: Eng*., **98**, 225-243.

Attia, A., Tounsi, A., Adda Bedia, E.A. and Mahmoud, S.R. (2015), "Free vibration analysis of functionally graded plates with temperature-dependent properties using various four variable refined plate theories", *Steel Compos. Struct*., **18**(1), 187-212.

Belabed, Z., Houari, M.S.A., Tounsi, A., Mahmoud, S.R. and Bég, O.A. (2014), "An efficient and simple higher order shear and normal deformation theory for functionally graded material (FGM) plates", *Compos.: Part B*, **60**, 274-283.

Beldjelili, Y., Tounsi, A. and Mahmoud, S.R. (2016), "Hygro-thermo-mechanical bending of S-FGM plates resting on variable elastic foundations using a four-variable trigonometric plate theory", *Smart Struct. Syst*., **18**(4), 755-786.

Belkorissat, I., Houari, M.S.A., Tounsi, A. and Hassan, S. (2015), "On vibration properties of functionally graded nano-plate using a new nonlocal refined four variable model", *Steel Compos. Struct*., **18**(4), 1063-1081.

Bellifa, H., Benrahou, K.H., Bousahla, A.A., Tounsi, A. and Mahmoud, S.R. (2017), "A nonlocal zeroth-order shear deformation theory for nonlinear postbuckling of nanobeams", *Struct. Eng. Mech*., **62**(6), 695 - 702.

Bellifa, H., Benrahou, K.H., Hadji, L., Houari, M.S.A. and Tounsi, A. (2016), "Bending and free vibration analysis of functionally graded plates using a simple shear deformation theory and the concept the neutral surface position", *J Brazil. Soc. Mech. Sci. Eng*., **38**(1), 265-275.

Bennoun, M., Houari, M.S.A. and Tounsi, A. (2016), "A novel five variable refined plate theory for vibration analysis of functionally graded sandwich plates", *Mech. Adv. Mater. Struct*., **23**(4), 423-431.

Bessaim, A., Houari, M.S.A. and Tounsi, A. (2013), "A new higher-order shear and normal deformation theory for the static and free vibration analysis of sandwich plates with functionally graded isotropic face sheets", *J. Sandw. Struct. Mater*., **15**(6), 671-703.

Besseghier, A., Houari, M.S.A., Tounsi, A. and Hassan, S. (2017), "Free vibration analysis of embedded nanosize FG plates using a new nonlocal trigonometric shear deformation theory", *Smart Struct. Syst.*, **19**(6), 601 - 614.

Boadu, K.B., Antwi-Boasiako, C. and Frimpong-Mensah, K. (2017), "Physical and mechanical properties of Klainedoxa gabonensis with engineering potential", *J. Forest. Res*., 28(3), 629-636.

Bouafia, Kh., Kaci, A., Houari M.S.A. and Tounsi, A. (2017), "A nonlocal quasi-3D theory for bending and free flexural vibration behaviors of functionally graded nanobeams", *Smart Struct. Syst*., **19**, 115-126.

Bouderba, B., Houari, M.S.A. and Tounsi, A. (2013), "Thermomechanical bending response of FGM thick plates resting on Winkler-Pasternak elastic foundations", *Steel Compos. Struct*., **14**(1), 85-104.

Bouderba, B., Houari, M.S.A., Tounsi, A. and Mahmoud, S.R. (2016b), "Thermal stability of functionally graded sandwich plates using a simple shear deformation theory", *Struct. Eng. Mech*., **58**(3), 397-422.

Boukhari, A., Atmane, H.A., Tounsi, A., Adda Bedia, E.A. and Mahmoud, S.R. (2016), "An efficient shear deformation theory for wave propagation of functionally graded material plates", *Struct. Eng. Mech.*, **57**(5), 837-859.

Bounouara, F., Benrahou, K.H., Belkorissat, I. and Tounsi, A. (2016), "A nonlocal zeroth-order shear deformation theory for free vibration of functionally graded nanoscale plates resting on elastic foundation", *Steel Compos. Struct*., **20**(2), 227-249.

Bourada, M., Kaci, A., Houari, M.S.A. and Tounsi, A. (2015), "A new simple shear and normal deformations theory for functionally graded beams", *Steel Compos. Struct*., **18**(2), 409-423.

Bousahla, A.A., Benyoucef, S., Tounsi, A. and Mahmoud, S.R. (2016a), "On thermal stability of plates with functionally graded coefficient of thermal expansion", *Struct. Eng. Mech.*, **60**(2), 313-335.

Cao, V.V. and Ronagh, H.R. (2014), "Reducing the potential seismic damage of reinforced concrete frames using plastic hinge relocation by FRP", *Compos. Part B: Eng*., **60**, 688-696.

Changwang, Y., Jinqing, J. and Ju, Z. (2010), "Seismic behavior of steel reinforced ultra high strength concrete column and reinforced concrete plate connection", *Trans. Tianjin Univ*., **16**, 309-316.

Cheng, C. and Chen, C. (2004), "Seismic behavior of steel plate and reinforced concrete column connections", *J. Constr. Steel Res*., **61**, 587-606.

Chikh, A., Tounsi, A., Hebali, H. and Mahmoud, S.R. (2017), "Thermal buckling analysis of cross-ply laminated plates using a simplified HSDT", *Smart Struct. Syst*., **19**(3), 289-297.

Choi, S.W., Yousok, K. and Park, H.S. (2014), "Multi-objective seismic retrofit method for using FRP jackets in shear-critical reinforced concrete frames", *Compos. Part B: Eng*., **56**, 207-216.

Davar, A., Khalili, S.M.R. and Malekzadeh Fard, K. (2013), "Dynamic response of functionally graded circular cylindrical shells subjected to radial impulse load", *Int. J. Mech. Mater. Des*., **9**, 65-81.

Draiche, K., Tounsi, A. and Mahmoud, S.R. (2016), "A refined theory with stretching effect for the flexure analysis of laminated composite plates", *Geomech. Eng*., **11**, 671-690.

Duc, N.D., Cong, P.H., Tuan, N.D., Tran, P. and Van Thanh, N. (2017a), "Thermal and mechanical stability of functionally graded carbon nanotubes (FG CNT)-reinforced composite truncated conical shells surrounded by the elastic foundation", *Thin Wall. Struct*., **115**, 300-310.

Duc, N.D., Hadavinia, H., Van Thu, P. and Quan, T.Q. (2015), "Vibration and nonlinear dynamic response of imperfect three-

phase polymer nanocomposite panel resting on elastic foundations under hydrodynamic loads", *Compos. Struct.*, **131**, 229-237.

Duc, N.D., Lee, J., Nguyen-Thoi, T. and Thang, P.T. (2017b), "Static response and free vibration of functionally graded carbon nanotube-reinforced composite rectangular plates resting on Winkler-Pasternak elastic foundations", *Aerosp. Sci. Technol*., **68**, 391-402.

Duc, N.D., Seung-Eock, K., Quan, T.Q., Long, D.D. and Anh, V.M. (2018), "Nonlinear dynamic response and vibration of nanocomposite multilayer organic solar cell", *Compos. Struct*., **184**, 1137-1144.

Duc, N.D., Tran, Q.Q. and Nguyen, D.K. (2017c), "New approach to investigate nonlinear dynamic response and vibration of imperfect functionally graded carbon nanotube reinforced composite double curved shallow shells subjected to blast load and temperature", *Aerosp. Sci. Technol*., **71**, 360-372.

El-Haina, F., Bakora, A., Bousahla, A.A. and Hassan, S. (2017), "A simple analytical approach for thermal buckling of thick functionally graded sandwich plates", *Struct. Eng. Mech*., **63**(5), 585-595.

Feng, Ch., Kitipornchai, S. and Yang, J. (2017), "Nonlinear bending of polymer nanocomposite plates reinforced with non-uniformly distributed graphene platelets (GPLs)", *Compos. Part B: Eng*., **110**, 132-140.

Formica, G., Lacarbonara, W. and Alessi, R. (2010), "Vibrations of carbon nanotube reinforced composites", *J. Sound Vib.*, **329**, 1875-1889.

GhorbanpourArani, A., Haghparast, E., Khoddami Maraghi, Z. and Amir, S. (2015), "Static stress analysis of carbon nano-tube reinforced composite (CNTRC) cylinder under non-axisymmetric thermo-mechanical loads and uniform electro-magnetic fields", *Compos. Part B: Eng*., **68**, 136-145.

JafarianArani, A. and Kolahchi, R. (2016), "Buckling analysis of embedded concrete columns armed with carbon nanotubes", *Comput. Concrete*, **17**, 567-578.

Ji, X., Zhang, M., Kang, H., Qian, J. and Hu, H. (2014), "Effect of cumulative seismic damage to steel tube-reinforced concrete composite columns", *Earthq. Struct*., **7**, 179-200.

Khetir, H., Bouiadjra, M.B., Houari, M.S.A., Tounsi, A. and Mahmoud, S.R. (2017), "A new nonlocal trigonometric shear deformation theory for thermal buckling analysis of embedded nanosize FG plates", *Struct. Eng. Mech*., **64**(4), 391-402.

Kolahchi, R., Rabani Bidgoli, M., Beygipoor, Gh. and Fakhar, M.H. (2013), "A nonlocal nonlinear analysis for buckling in embedded FG-SWCNT-reinforced microplates subjected to magnetic field", *J. Mech. Sci. Tech*., **5**, 2342-2355.

Kolahchi, R., Safari, M. and Esmailpour, M. (2016), "Dynamic stability analysis of temperature-dependent functionally graded CNT-reinforced visco-plates resting on orthotropic elastomeric medium", *Compos. Struct*., **150**, 255-265.

Larbi Chaht, F., Kaci, A., Houari, M.S.A. and Hassan, S. (2015), "Bending and buckling analyses of functionally graded material (FGM) size-dependent nanoscale beams including the thickness stretching effect", *Steel Compos. Struct*., **18**(2), 425 -442.

Lei, Z.X., Zhang, L.W., Liew, K.M. and Yu, J.L. (2014), "Dynamic stability analysis of carbon nanotube-reinforced functionally graded cylindrical panels using the element-free kp-Ritz method", *Compos. Struct*., **113**, 328-338.

Liang, X. and Parra-Montesinos, G.J. (2004), "Seismic behavior of reinforced concrete column-steel plate subassemblies and frame systems", *J. Struct. Eng*., **130**, 310:319.

Liew, K.M., Lei, Z.X., Yu, J.L. and Zhang, L.W. (2014), "Postbuckling of carbon nanotube-reinforced functionally graded cylindrical panels under axial compression using a meshless approach", *Comput. Meth. Appl. Mech. Eng*., **268**, 1-17.

Liu, Z.Q., Xue, J.Y. and Zhao, H.T. (2016), "Seismic behavior of steel reinforced concrete special-shaped column-plate joints", *Earthq. Struct*., **11**, 665-680.

Mahi, A., Bedia, E.A.A. and Tounsi, A. (2015), "A new hyperbolic shear deformation theory for bending and free vibration analysis of isotropic, functionally graded, sandwich and laminated composite plates", *Appl. Math. Model*., **39**, 2489-2508.

Matsuna, H. (2007), "Vibration and buckling of cross-ply laminated composite circular cylindrical shells according to a global higher-order theory", *Int. J. Mech. Sci.*, **49**, 1060-1075.

Mehri, M., Asadi, H. and Wang, Q. (2016), "Buckling and vibration analysis of a pressurized CNT reinforced functionally graded truncated conical shell under an axial compression using HDQ method", *Comput. Meth. Appl. Mech. Eng*., **303**, 75-100.

Menasria, A., Bouhadra, A., Tounsi, A. and Hassan, S. (2017), "A new and simple HSDT for thermal stability analysis of FG sandwich plates", *Steel Compos. Struct*., **25**(2), 157-175.

Meziane, M.A.A., Abdelaziz, H.H. and Tounsi, A.T. (2014), "An efficient and simple refined theory for buckling and free vibration of exponentially graded sandwich plates under various boundary conditions", *J. Sandw. Struct. Mater*., **16**(3), 293-318.

Mori, T. and Tanaka, K. (1973), "Average stress in matrix and average elastic energy of materials with misfitting inclusions", *Acta Metall. Mater.*, **21**, 571-574.

Mouffoki, A., Adda Bedia, E.A., Houari M.S.A. and Hassan, S. (2017), "Vibration analysis of nonlocal advanced nanobeams in hygro-thermal environment using a new two-unknown trigonometric shear deformation beam theory", *Smart Struct. Syst.*, **20**(3), 369 - 383.

Shen, H.S. and Yang, D.Q. (2014), "Nonlinear vibration of anisotropic laminated cylindrical shells with piezoelectric fiber reinforced composite actuators", *Ocean Eng.*, **80**, 36-49.

Shu, C. and Xue, H. (1997), "Explicit computations ofweighting coefficients in the harmonic differential quadrature", *J. Sound Vib*., **204**(3), 549-55.

Simsek, M. (2010), "Non-linear vibration analysis of a functionally graded Timoshenko plate under action of a moving harmonic load", *Compos. Struct*., **92**, 2532-2546.

Simsek, M. and Reddy, J.N. (2013), "A unified higher order plate theory for buckling of a functionally graded microplate embedded in elastic medium using modified couple stress theory", *Compos. Struct*., **101**, 47-58.

Thanh, N.V., Khoa, N.D., Tuan, N.D., Tran, P. and Duc, N.D. (2017), "Nonlinear dynamic response and vibration of functionally graded carbon nanotube-reinforced composite (FG-CNTRC) shear deformable plates with temperature-dependent material properties", *J. Therm. Stress*., **40**, 1254-1274.

Van Thu, P. and Duc, N.D. (2016), "Non-linear dynamic response and vibration of an imperfect three-phase laminated nanocomposite cylindrical panel resting on elastic foundations in thermal environment", *Sci. Eng. Compos. Mater*., **24**(6), 951-962.

Wuite, J. and Adali, S. (2005), "Deflection and stress behaviour of nanocomposite reinforced plates using a multiscale analysis", *Compos. Struct*., **71**, 388-396.

Zemri, A., Houari, M.S.A., Bousahla, A.A. and Tounsi, A. (2015), "A mechanical response of functionally graded nanoscale beam: an assessment of a refined nonlocal shear deformation theory beam theory", *Struct. Eng. Mech*., **54**(4), 693-710.

Zidi, M., Tounsi, A. and Bég, O.A. (2014), "Bending analysis of FGM plates under hygro-thermo-mechanical loading using a four variable refined plate theory", *Aerosp. Sci. Tech.*, **34**, 24-34.

CC